

Dielectric resonance bandgap and localized defect mode in a periodically ordered metallic-dielectric composite

Ying Gu* and Qihuang Gong[†]*State Key Laboratory for Mesoscopic Physics, Department of Physics, Peking University, Beijing 100871, China*

(Received 11 March 2004; published 2 September 2004)

Dielectric resonance bandgap and localized defect mode in the periodically ordered metallic-dielectric composite networks are investigated by the Green's function formalism. Several band gaps with the zero density of states are shown in the spectrum of dielectric resonances. We find that most of the eigenmodes have an extended field distribution, which is represented by the inverse participation ratio (IPR). Moreover, the defect modes with high values of IPR are fallen into the resonance bandgaps and their positions are very sensitive to the admittance of the defect. The field of these defect modes is very localized around the defect. Finally, we discuss the influence of defect modes to the optical responses.

DOI: 10.1103/PhysRevB.70.092101

PACS number(s): 42.70.Qs, 61.72.-y, 77.84.Lf

Periodical structure of crystals leads to the bandgap of electron energy controlling the conductivity of certain materials. Following this, a semiconductor is fabricated. In the periodically ordered dielectric structure or a photonic crystal, photonic bandgaps are used to tailor the properties of light, namely, some frequencies of lights can transmit the materials while others are completely forbidden.¹ In the locally resonant sonic crystals, there exist spectral gaps that forbid some frequencies acoustic wave propagation.² Therefore, the periodical arrays always suppress some of the eigenmodes, while enhance others, forming the bandgap of the eigenmodes. Based on this idea, in this paper, the properties of dielectric resonances in the periodically arranged metallic-dielectric nano-structure composite are investigated.

Recently, people start to study the properties of metallic photonic crystals possessing the negative dielectric constant or metallic components.³⁻⁵ Various metallic-dielectric photonic crystals are fabricated.^{6,7} The bandgaps of transmittance spectrum and the defect mode are very different from the general photonic crystal where only the positive dielectric constants exist.⁸⁻¹¹ For the composite materials, there are some quasistatic dielectric resonances due to the simultaneously existing positive and negative admittance.^{12,13} When resonance happens, the fields are localized within or around the impurity metallic clusters.¹⁴⁻¹⁶ These resonances were found not only in the isolated clusters,¹⁴⁻¹⁶ but also in various disordered composites,^{17,18} and in the periodically structured nanometer materials.³ In the present, instead of the bandgap of light transmittance, we study the bandgap of dielectric resonance in a periodically ordered metallic-dielectric composite network.

To model the resonant properties of composite materials, we developed Green's function formalism (GFF) in a binary and three-component network.^{14,17} GFF is used to calculate the resonance spectrum and local field distribution at resonance for a cluster with arbitrary geometry embedded in the infinite network, as well as for a periodically ordered metallic-dielectric composite. Consider a binary square network, where the impurity metallic clusters with the admittance ϵ_2 in each bond are embedded in the otherwise homogeneous infinite networks with the admittance ϵ_1 in each

bond. The Kirchhoff equations of electrostatic Green's function $F_{\mathbf{x},0}$ reads¹⁴

$$\sum_{\mathbf{y}(\mathbf{x})} \epsilon_{\mathbf{x},\mathbf{y}} (F_{\mathbf{x},0} - F_{\mathbf{y},0}) = \delta_{\mathbf{x},0}, \quad (1)$$

with the admittance $\epsilon_{\mathbf{x},\mathbf{y}} = \epsilon_{\mathbf{y},\mathbf{x}}$. The microstructure of impurity metallic clusters is completely mapped by the Green's matrix \tilde{M} in the clusters subspace, where $\tilde{M}_{\mathbf{x},\mathbf{y}} = \sum_{\mathbf{z} \in C(\mathbf{y})} (G_{\mathbf{x},\mathbf{y}} - G_{\mathbf{x},\mathbf{z}})$ and $G_{\mathbf{x},\mathbf{y}}$ is the Green's function of Laplace operator on the infinite square. The eigenvalues $s (= 1/(1 - \epsilon_2/\epsilon_1))$ of \tilde{M} form the dielectric resonance spectrum. Dielectric resonances (or eigenvalues of \tilde{M}) are independent of the external sources, but closely related to the geometric structure of impurities, so they are also called geometric resonances. In a binary metallic-dielectric network, the resonances lie in the range¹² $0 \leq s \leq 1$.

Since \tilde{M} maps the microstructure of the impurity metallic clusters and its eigenvalues determines the values of resonances, these dielectric resonances are also called geometric resonances. For the random composites, the elements of \tilde{M} are randomly distributed. The level spacings of their eigenvalues (or resonances) obey the poisson distribution for the very dilute composites and Gaussian distribution for the percolating composites.¹⁸ However, due to the periodical structure of the impurity admittance ϵ_2 , there exists many equal elements in \tilde{M} , so the symmetry of \tilde{M} is modified. Now, the distribution of the dielectric resonances does not obey the laws of random matrix theory. And the modification of \tilde{M} suppresses some dielectric resonances, while densifies others, leading to the occurrence of the resonance bandgaps.

As shown in Fig. 1, the periodically ordered impurity metallic arrays with the admittance ϵ_2 in each bond are embedded in an otherwise homogeneous dielectric network with admittance ϵ_1 , forming a two-dimensional (2D) metallic-dielectric array. Instead of the transmittance properties, here we discuss its dielectric resonance in the quasistatic limit. In a 2D square network, several one-dimensional (1D) metallic-dielectric arrays are checked, but no dielectric resonance bandgap is found. In the 2D arrays, we noted that for the

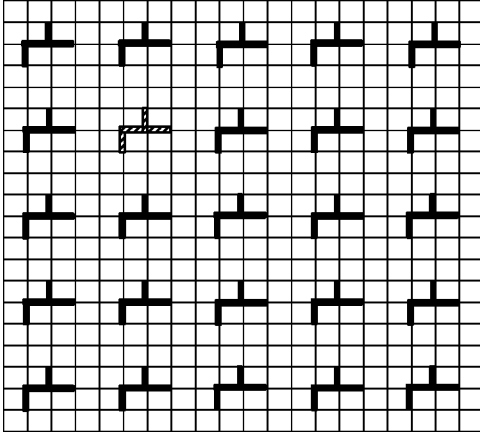


FIG. 1. Schematic diagram of a periodically arranged metallic-dielectric array. The defect cell is marked by the stripes.

symmetric unit cell only three resonance bandgaps are shown. While, in Fig. 1, the highly unsymmetric unit cell is chosen and five resonance bandgaps are obtained. Further numerical calculations indicate that the bandgap of dielectric resonances still exist in the 2D photonic crystals, where the dielectric constants has two dimensional periodicity but the structure is in fact three dimensional. In this figure, the interval of each unit cell at two directions is 4 bonds. For a 5×5 periodical metallic-dielectric array, there are 25 cells, totally 100 metallic bonds. So except the trivial eigenvalues 0 and 1, there are 100 nontrivial resonances within $(0, 1)$. Our numerical calculations also indicate that the symmetry of unit cell and the interval among the cells determine the number and width of the bandgaps.

For a 5×5 periodical metallic-dielectric array shown in Fig. 1, we calculate the density of eigenstates (DOS) of these 100 dielectric resonances. We set the interval of resonances $\Delta s = 0.02$ and the statistics region $s \in (0, 1)$. As shown in Fig. 2, from 0 to 1, we find 5 resonance bandgaps with the zero DOS in the resonance spectrum. The first gap is started from the zero and the largest gap is ended to 1.0. The largest bandgap is from $s = 0.3340$ to $s = 0.5765$. The relation $\Sigma \Delta s \cdot \text{DOS} = 1$ is satisfied. For a random composite, the resonances are randomly distributed within the area $s \in (0, 1)$ and level spacing of resonances has the general statistical

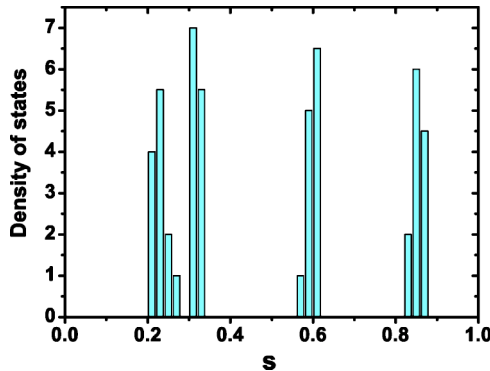


FIG. 2. Density of states of dielectric resonances for a 5×5 array. The statistical interval is $\Delta s = 0.02$.

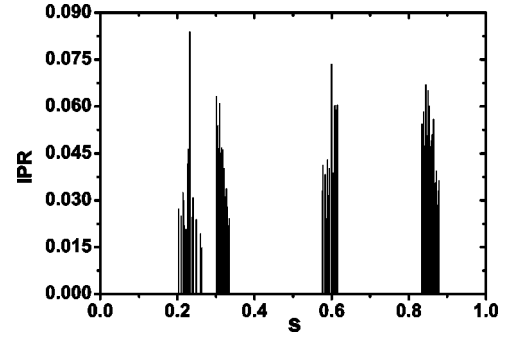


FIG. 3. IPR of the right eigenvectors for a 5×5 array.

features.¹⁸ While, for a periodically ordered metallic-dielectric structure, in the quasistatic limit, we find the dielectric resonance bandgap.

When dielectric resonance happens, the local field is localized within and around the impurity metallic arrays. We employ the residue of the electrical potential to remove the infiniteness. Near resonance, it reads¹⁴

$$\text{Residue}(F_{x,0}) = \frac{1}{\epsilon_2} \left(\sum_{y \in C} \tilde{L}_{m,y} \tilde{G}_{y,0} \right) \left(\sum_{z \in C} M_{x,z} \tilde{R}_{m,z} \right), \quad (2)$$

where \tilde{R}_m and \tilde{L}_m are the m th normalized right and left eigenvectors of the Green's matrix \tilde{M} , and $M_{x,z} = \sum_{y \in C(z)} (G_{x,z} - G_{x,y})$. We use the inverse participation ratio (IPR)¹⁹ of right eigenvector to represent the local field distribution of each resonance. The calculation of $\text{IPR}(R_n)$ is limited in the nontrivial eigenstates. Instead of the transmittance of light in a photonic crystal, here for each resonance, IPR is used to represent the localization of field. Figure 3 displays the IPRs of right eigenvectors of the above 5×5 metallic-dielectric array. It is seen that most of IPRs are distributed within the values $(0.015, 0.060)$, belonging to the same order. While, in the percolating composite network, the values of IPR are distributed in the large period and are more randomly.²⁰ It implies that in a periodically ordered metallic-dielectric array the local fields near resonances have about the same degree of localization. Then, for a 5×5 metallic-dielectric array with 100 dielectric resonances, we have checked the local field distribution of about 20 resonances. Numerical calculations indicate that most of the eigenmodes have the extended local field. To have an instructive description, using Eq. (2), we calculate residues of the typical local field distribution and illustrate it by a three-dimensional (3D) plot, as shown in Fig. 4, where $s = 0.3073$ and the corresponding $\text{IPR} = 0.04592$. We observe that the local field is almost uniformly extended in the whole sample. In a random composite, local field at resonance is either localized within a small area, say a "hot spot," or uniformly extended through the whole sample.^{16,20} We note that at $\text{DOS} = 0$ the local field is not zero, but a superposition of all the eigenmodes, calculated by Eq. (16) in Ref. 14.

In a photonic crystal, due to the impurities, the defect modes are fallen into the photonic bandgap.¹ These kinds of defect modes are also reported in a metallic photonic crystal.²¹ Then, in view of dielectric resonances, how about

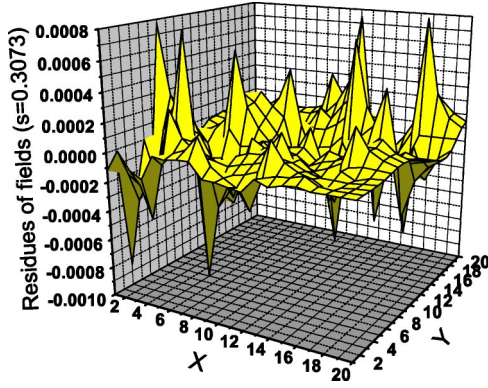


FIG. 4. Typical local field distribution near resonances. Here $s=0.3073$ and the corresponding $IPR=0.04592$.

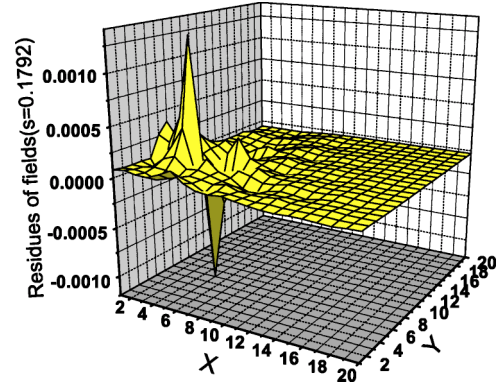


FIG. 6. Typical local field distribution of a defect mode. Here $\eta=0.6$, $s=0.1792$, and $IPR=0.27323$.

the defect modes of a metallic photonic crystal? In a 5×5 metallic-dielectric array, a defect with admittance ϵ_3 in each bond is shown as stripes in Fig. 1. Instead of directly changing ϵ_3 , we introduce the difference admittance ratio η ,¹⁷ defined as $\eta=(\epsilon_3-\epsilon_1)/(\epsilon_2-\epsilon_1)$. When $\eta=1$, no defect exists. Figure 5 displays the defect modes of dielectric resonance with $\eta=0.5$ and $\eta=0.6$. Because each unit cell includes 4 metallic bonds, for each case, 4 defect modes are shown in the bandgap of dielectric resonances. We find that these defect modes have very large values of IPR, i.e., these eigenmodes possess a very localized field distribution. For a fixed η , when we move the defect from the corner to center, no obvious change is observed in the IPR spectrum. However, the positions of defect modes are very sensitive to admittance of the defect. The results are shown in Fig. 5(a) with $\eta=0.5$ and Fig. 5(b) with $\eta=0.6$. The small change of η makes the 3rd defect modes jump from the 2nd bandgap into the 3rd one. Correspondingly, this defect only has a very weak influence to the IPR of other eigenmodes.

Then, we investigate the local field distribution of defect modes for $\eta=0.5$ and $\eta=0.6$. For these 8 defect modes, we

find that the field is localized within and around the defect. While, away from the defect, the field is very smoothly distributed. In a random composite, we also reported the very localized field distribution or a “hot spot.”^{16,20} However, away from the “hot spot,” the field is extended,²⁰ not smooth. Figure 6 displays the local field distribution of a typical defect mode for $\eta=0.6$, where $s=0.1792$ and $IPR=0.27323$. Compared to Fig. 4, the field of a defect mode is very localized within a small area, but do not have a high intensity. So a single defect may not have much influence on the optical properties of the whole metallic-dielectric array.

Consider a metallic-dielectric array in an infinite square network with a point source $(0,0)$, the effective linear and nonlinear optical responses are given by²² $\epsilon_e=\sum_\alpha \epsilon_\alpha |\partial F_\alpha|^2$ and $\chi_e=\sum_\alpha \chi_\alpha |\partial F_\alpha|^4$. The coefficients ϵ_e and χ_e indicate that, when resonance happens, how the energy are concentrated in the impurity metallic clusters. We employ Drude free electronic model to compute the optical responses of a metallic photonic crystal. The admittance ϵ_2 of the impurity metallic bonds is defined as $\epsilon_2=1-[\omega_p^2/\omega(\omega+i\gamma)]$, where $\omega_p \approx 10^{16}$ is the plasma frequency, $\gamma=0.01\omega_p$ a damping constant and $\epsilon_1=1.77$. The defect admittance ϵ_3 is given by the relation $\epsilon_2=\epsilon_0+\eta(\epsilon_1-\epsilon_0)$.¹⁷ In Fig. 7, only the effective linear responses are considered, and the similar features as shown in the nonlinear responses.

Figure 7 displays the imaginary part (or absorption) of effective linear optical responses of a 5×5 metallic-dielectric array for the different admittance ratio η . The solid curve illustrates the optical responses of a metallic photonic crystal without the defect, i.e., $\eta=1$. While the dotted and dashed curves give the optical responses of the metallic-dielectric array with a single defect for $\eta=0.5$ and $\eta=0.6$, respectively. It is shown that 5 bandgaps of dielectric resonances are separated by several absorption peaks. There is a proper correspondence between the IPR of right eigenvectors and the optical responses. For $\eta=0.5$, we observe the weak optical responses corresponding to the defect modes $s=0.1517$ and $s=0.4282$. As well as for $\eta=0.6$, the optical responses of defect modes are obtained at $s=0.1792$, $s=0.3650$ and $s=0.5124$. At last, due to the influence of defect modes, the intensity of each absorption peak has very little change, as expected from its local field distribution.

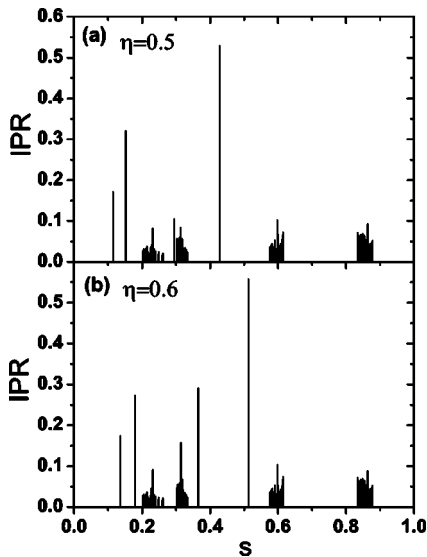


FIG. 5. The localized defect modes for (a) $\eta=0.5$ and (b) $\eta=0.6$.

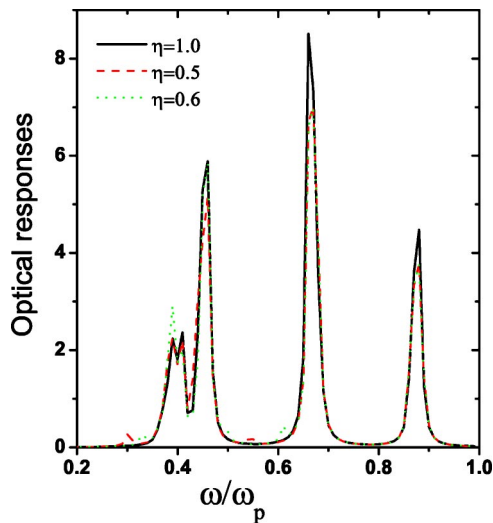


FIG. 7. The imaginary parts of the effective linear optical responses for a 5×5 array. The calculations are modeled by the Drude model. Here $\eta = 1.0, 0.5,$ and 0.6 .

It is known that for $\eta = 0.5$ and 0.6 the value of dielectric resonance is still limited in the interval $(0, 1)$. However, when η is negative or is much larger than 1, the range of dielectric resonances will become wide. Correspondingly, the defect modes with negative η or large η will have a different

effect in the IPR spectrum and in the optical responses. Moreover, if the cell defect is replaced by a line defect or others, the defect modes will modify the IPR of right eigenmodes and optical responses very well.

In summary, we first investigate the dielectric resonance bandgap and defect mode in a periodically ordered metallic-dielectric composite network. Using Green's function formalism, we have found several band gaps with the zero density of states in the resonance spectrum, as well as in the inverse participation ratios (IPR) representing the local field distribution of eigenstates. The localized defect modes are shown in the IPR spectrum and their positions are very sensitive to the admittance of the defect. Finally, for a single cell defect, we discuss the influence of defect modes to the optical responses.

The work was supported by National Natural Science Foundation of China under Grant Nos. 10304001, 10334010, 10328407, and 90101027. It was also supported by the special fund from Ministry of Science and Technology of China, the National Key Basic Research Special Foundation under Grant No. TG1999075207, and partly sponsored by the Scientific Research Foundation for the Returned Overseas Chinese Scholars, State Education Ministry. We thank Professor Z. R. Yang, Professor H. B. Jiang, and Professor J. S. Zhang for the discussions and B. Dai for numerical calculations in 3D.

*Email address: ygu@pku.edu.cn

†Email address: qhgong@pku.edu.cn

¹K. Sakoda, *Optical Properties of Photonic Crystals* (Springer series in optical sciences, 2001).

²Z. Y. Liu *et al.*, *Science* **289**, 1734 (2000).

³D. F. Sievenpiper, E. Yablonovitch, J. N. Winn, S. Fan, P. R. Villeneuve, and J. D. Joannopoulos, *Phys. Rev. Lett.* **80**, 2829 (1998).

⁴S. Y. Lin *et al.*, *Nature (London)* **394**, 251 (1998).

⁵J. G. Fleming *et al.*, *Nature (London)* **417**, 52 (2002).

⁶F. Li *et al.*, *Adv. Mater. (Weinheim, Ger.)* **14**, 1528 (2002).

⁷G. S. Cheng and M. Moskovits, *Adv. Mater. (Weinheim, Ger.)* **14**, 1567 (2002).

⁸T. W. Ebbesen *et al.*, *Nature (London)* **391**, 667 (1998).

⁹C. J. Jin *et al.*, *Appl. Phys. Lett.* **75**, 1201 (1999).

¹⁰A. Moroz, *Phys. Rev. B* **66**, 115109 (2002).

¹¹J.-M. Lourtioz and A. De Lustrac, *C. R. Phys.* **3**, 79 (2002).

¹²For a review, see D. J. Bergman and D. Stroud, in *Solid State*

Physics, edited by H. Ehrenreich and D. Turnbull (Academic, New York, 1992), Vol. 146, p. 147.

¹³J. P. Clerc, G. Giraud, J. M. Luck, and Th. Robin, *J. Phys. A* **29**, 4781 (1996).

¹⁴Y. Gu, K. W. Yu, and H. Sun, *Phys. Rev. B* **59**, 12847 (1999).

¹⁵M. I. Stockman, *Phys. Rev. E* **56**, 6494 (1997).

¹⁶A. K. Sarychev, V. A. Shubin, and V. M. Shalaev, *Phys. Rev. B* **60**, 16389 (1999).

¹⁷Ying Gu and Qihuang Gong, *Phys. Rev. B* **67**, 014209 (2003).

¹⁸Y. Gu, K. W. Yu, and Z. R. Yang, *Phys. Rev. E* **65**, 046129 (2002).

¹⁹F. Wegner, *Z. Phys. B* **36**, 209 (1980).

²⁰Y. Gu, K. W. Yu, and Z. R. Yang, *Phys. Rev. B* **66**, 012202 (2002).

²¹T. Ochiai and J. Sanchez-Dehesa, *Phys. Rev. B* **65**, 245111 (2002).

²²D. Stroud and P. M. Hui, *Phys. Rev. B* **37**, 8719 (1988).